Archives of Materials Science and Engineering

Volume 106
Issue 2
December 2020
Pages 68-77

International Scientific Journal
published monthly by the
World Academy of Materials
and Manufacturing Engineering

DOI: 10.5604/01.3001.0014.6974

CO_2 laser spot welding of thin sheets AISI 321 austenitic stainless steel

A.A. Shehab [a], S.A. Nawi [a], A. AAG Al-Rubaiy [a,*], Z. Hammoudi [b], S.A. Hafedh [c], M.H. Abass [d], M.S. Alali [e], S.D. Ali [b]

[a] Department of Materials Engineering, University of Diyala, Diyala, Iraq
[b] Department of Mechanical Engineering, University of Diyala, Diyala, Iraq
[c] Department of Electrical Power and Machines Engineering, University of Diyala, Diyala, Iraq
[d] Ministry of Oil, Midland Oil Company, Baghdad, Iraq
[e] Department of Materials Engineering, University of Kufa, Najaf, Iraq
* Corresponding e-mail address: ghaidan3@yahoo.com
ORCID identifier: https://orcid.org/0000-0002-3331-321X (A.AAG A.-R.)

ABSTRACT

Purpose: The present work aims to investigate the influence of CO_2 laser spot welding (LSW) parameters on welding profile and mechanical properties of lap joint of AISI 321 thin sheet metals, and analyze the welding profile numerically by finite element (FE) method.

Design/methodology/approach: The weld carried out using 150 W CO_2 continues wave laser system. The impact of exposure time and laser power on the welding profile was investigated using an optical microscope. Microhardness and tensile strength tests were used to evaluate the mechanical properties of the joint. Ansys software was utilized to simulate the welding profile numerically.

Findings: The results revealed that 2 s exposure time and 50 W power have led to uniform welding profile and highest shear force (340 N), lower hardness gradient across the heat affected zone (HAZ) and fusion zone (FZ). Finite element (FE) analysis of the welding profile showed good agreement with experimental analysis.

Research limitations/implications: The selection of laser spot welding parameters for thin sheet metal was critical due to the probability of metal vaporisation with extra heat input during welding.

Practical implications: Laser welding of AISI 321 steel is used in multiple industrial sectors such as power plants, petroleum refinement stations, pharmaceutical industry, and households. Thus, selecting the best welding parameters ensures high-quality joint.

Originality/value: The use of CO_2 laser in continuous wave (CW) mode instead of pulse mode for spot welding of thin sheet metal of AISI 321 austenitic stainless steel consider a real challenge because of the difficulty of control the heat input via proper selection of the welding parameters in order to not burn the processed target. Besides, the maintenance is easier and operation cost is lower in continuous CO_2 than pulse mode.

Keywords: Thin sheet metal, Austenitic stainless steel, CO_2 CW LSW, Mechanical properties, Welding profile, FE analysis

Reference to this paper should be given in the following way:
A.A. Shehab, S.A. Nawi, A. AAG Al-Rubaiy, Z. Hammoudi, S.A. Hafedh, M.H. Abass, M.S. Alali, S.D. Ali, CO_2 laser spot welding of thin sheets AISI 321 austenitic stainless steel, Archives of Materials Science and Engineering 106/2 (2020) 68-77.
DOI: https://doi.org/10.5604/01.3001.0014.6974

1. Introduction

In various industries, products such as heat exchangers, membranes, fastening elements contain parts made with thin-walled designs of thicknesses usually from 0.2 to 0.6 mm. These parts are usually manufactured by welding sheets of stainless steels [1].

Austenitic stainless steels are a good candidate for many applications [2-4] due to its high corrosion resistance. Intergranular corrosion of welded joints in austenitic steels is one of these problems and can be prevented by reduction of carbon content in steels and consumables below 0.03% [1]. The low thermal conductivity (15.5 W/m·K) and high thermal expansion ($18x10^{-6}$ 1/K) of austenitic stainless steels have a significant drawback in welding especially in the case of welding thin sheets by raising the probability of thermal distortions [5-7].

Welding of thin sheet metals requires a good control to the heat input during welding process [8,9]. They have been indicated in literatures that the essential condition for ensuring integrity welding in austenitic stainless steel is reducing the heat input of welding, which can be guaranteed by high power density welding process such laser beam welding and electron beam welding [5,6] Thus, there is a great challenge in choosing of best welding processing parameters such as exposure time, power, beam diameter, lens focal length, focus arrangement concerning the machinable surface.

Among austenitic stainless steels series, AISI 321 welding by laser beam welding process has received important concern in industry due to its significant usage in high pressure tanks for transportation of liquids and compressed gases, in power plants and petroleum refinement stations. Existing of Ti in the chemical composition of AISI 321 is useful in enhancing the resistance to surface oxidation. Besides, preventing the inter-granular corrosion and chromium carbide precipitation at the grain boundary during welding [10].

Many studies were carried out to investigate the welding of AISI 321stainless steel with small thickness. A. Klimpel and A. Lisiecki [11] have computed the welding parameters that ensures joint strength to be higher than the strength of the base material (BM) and high quality joint, without any defects, during diode laser welding of AISI 321 sheets of 0.5 and 1.0 mm thick.

Elena Manuela et al. [12] have studied the hardness profile and tensile strength of laser dissimilar welding of AISI 321 sheets to AISI 1010 carbon steel using diode laser.

The hardness is calculated by the amount of iron diffused from carbon steel, which, with the alloying elements, could form intermetallic phases such as FeNi and CrNiFe, contributing to an overall increase in hardness. The results also showed that the dissimilar welding joints present strong tensile behaviour with an ultimate tensile strength comparable to the mechanical characteristics of carbon steel.

A. Hussain et al. [13] have investigated the effect of CO_2 laser welding on joint strength and hardness of AISI 321 sheets. It was observed that mechanical properties of laser welded butt joints of austenitic steel sheets are almost similar to the base metal.

The impact of Pulse fiber laser parameters on mechanical properties of AISI 321 to AISI 405 stainless steel dissimilar joint was studied by Wei Meng et al. [14] The results showed that excellent joints were produced at a frequency of 400-600 Hz where the tension samples broke near the fusion boundary at AISI 405 HAZ. The microhardness of the weld zone was substantially higher than that of other heat affected zone and the substrates.

Laser spot welding (LSW) is getting increasing observation as a high speed technique to substitute the resistance spot welding process for welding thin sheet metal in many industries [15-17]. Up to date, CO_2 LSW for austenitic stainless steel thin sheets has not been sufficiently investigated in the literature due to high quantity of heat concentration in the weld zone, which can lead to welding distortion [1, 18]. Therefore, the use of continuous wave (CW) laser needs careful selection of welding parameters. The present study investigated the effect of 150 W CO_2 CW laser exposure time and laser power on the welding profile and mechanical properties (shear strength and micro-hardness) during spot welding of 0.2 mm thickness AISI 321austenitic stainless steel sheets. Welding profile was analyzed numerically by finite element FE method using Ansys 15 software.

2. Materials and methods

The welding was performed on 10×100×0.2 mm sheets of AISI 321 austenitic stainless steel. The chemical composition (shown in Tab. 1) was analyzed using spectromax device (manufactured by Ametek company, Germany). Mechanical properties and thermophysical properties for the selected materials are presented in Tables 2 and 3 respectively.

The welding experiments were carried using 150 W CO_2 CW laser system university made. The selection of welding parameters (listed in Tab. 4) was based on literature [18] beside several preliminary experimental tests. The input variables of the welding experiments included laser exposure time and laser power. Gradual increase of the exposure time while keeping power constant and vice versa, was utilized to investigate the impact of the parameters on the joint mechanical properties. The focusing lens has 63 mm focal length that produced ~600 μm spots size. Laser spot size at the surface of the target was about 800 μm.

Prior welding, the surfaces of the sheets were ground with 400 grits SiC papers to reduce the reflectivity of the surface of the sheet and degreased by acetone to ensure clean surface that is free of dirt. The sheets were positioned and fastened using a specially designed clamping device. The laser system, experimental setup and joint assembly of this study are presented in Figure 1.

Table 1.
Chemical composition of AISI 321 stainless steel

Element, wt.%	C	Mn	Si	P	S	Cr	Ni	Ti
AISI 321	0.10	2	0.75	0.04	0.03	17	9.00	0.15

Table 2.
Mechanical properties of AISI 321 stainless steel [10]

Tensile strength, MPa	0.2%Yield strength, MPa	Elongation, %	Hardness, HV
515	205	40	175

Table 3.
Thermophysical properties of AISI 321 grade stainless steel [10]

Thermal conductivity, k, W/m.K	Specific heat, c, J/kg.K	Density, ρ, Kg/m³	Thermal diffusivity, β, mm²/s	Melting temperature, T_m, ºC	Evaporating temperature, T_v, ºC	R%, reflectivity at 27ºC	R%, reflectivity at T_m
20.50	500	7900	5.19	1430	3027	90.30	86

Table 4.
The operating welding parameters for the present work with breaking shear force

Sample No.	Laser power, W	Laser exposure time, s	Breaking shear force, N
1	50	1.4	50
2	50	1.6	243
3	50	1.8	300
4	50	2	340
5	40	2	290
6	60	2	260
7	70	2	200
8	80	2	80

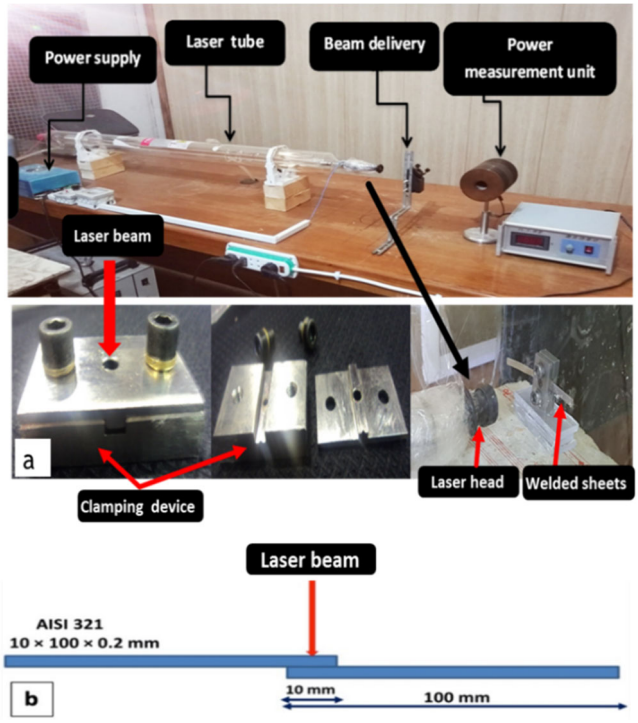

Fig. 1. (a) Laser system and experimental set up of this study (b) A schematic representation of lap joint assembly

Mechanical properties were evaluated using a universal testing machine type SANTAM model STM-20. The welded samples were cut and prepared for microstructural observation using a standard grinding and polishing method. To reveal the details of the joint microstructure, etching was conducted for 30 s with fresh reagent that consists a mixture of equal amount of three acids (HCL, HNO_3 and acetic acid). Optical microscope V83MC50 (China) inspected the geometry and microstructure of the joints. Digital Micro-Vickers Hardness Tester model no. (HVS-1000/China) was used to determine Vickers micro-hardness. Loading force was 4.9 N was applied for 15 s. Average of more than two computations was documented for different positions through the joint including BM, HAZ and FZ.

3. Finite element analysis

The problem was analyzed numerically by finite element method using Ansys 15 software. The aim is to estimate the temperature distribution in the welding zone at the end of the laser shot and then comparing with the real welding profile to validate the simulation.

3.1. Geometrical considerations for FE modelling

The geometry of the mounting frame is shown in Figure 2. Since the diameter of the laser beam is very small compared to the dimensions of the mounting frame, and the time of transient heat transfer is very short, the axisymmetric model is adopted for the analysis.

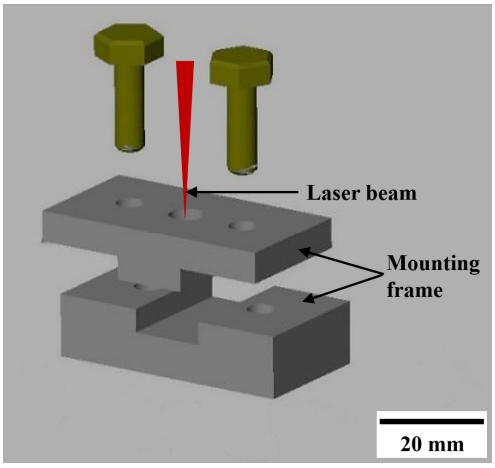

Fig. 2. The mounting frame for laser welding used in this study

The central axis of the laser beam is assumed as the axis of symmetry. A plane slice, passing through it containing the welded plates and the mounting frame, is modelled. The width and height of this slice are taken far enough from the axis of symmetry and heat source.

Element type Plane55 with square shape is used to model the contacting plates and the mounting frame. The fine sized mesh is used near the area of applied laser power because of the high thermal gradient in this region. Conta172 and Targe169 elements, are used to model the contact regions between plates and the mounting frame. The thermal contact conductance between contacting surfaces is taken into account in the analysis. The value of the factor of this contact conductance depends on several factors such as materials, surface finish, and contact pressure between the contacting bodies, it can't be computed analytically, but can be estimated experimentally. Transient heat transfer analysis is carried out during the period of laser application. Adaptive time-stepping is implemented in Ansys.

3.2. Theoretical formulation

According to 1st law of thermodynamics, the equation for heat flow in 3D solid can be written as follow [19]:

$$\rho \frac{\partial}{\partial t} \int_{To}^{T} c(T)\, d\, T = \frac{\partial}{\partial x}\left[k(T)\frac{\partial T}{\partial x}\right] + \frac{\partial}{\partial y}\left[k(T)\frac{\partial T}{\partial y}\right] + \frac{\partial}{\partial z}\left[k(T)\frac{\partial T}{\partial z}\right] = Q(x,y,z,t) \quad (1)$$

where ρ is material's density, c (T) and k (T) are the material temperature-dependent specific heat and thermal conductivity respectively, $Q(x,y,z,t)$ is the rate at which heat is supplied to solid, per unit time, per unit volume, T=T(x,y,z,t) is the resulting 3D time-dependent temperature distribution in the material, t is the time, T_0 is the initial temperature, x, y, z are the Cartesian coordinates. For this study, it is assumed that k (T) and c (T) do not change dramatically with T, so they are considered constant for a particular time interval. For the current study, the transient heat transfer analysis is considered along transverse section as shown in Figure 3, where the yellow parts represents the mounting frame (Fig. 2) that cut from axis of symmetry along the laser beam inlet.

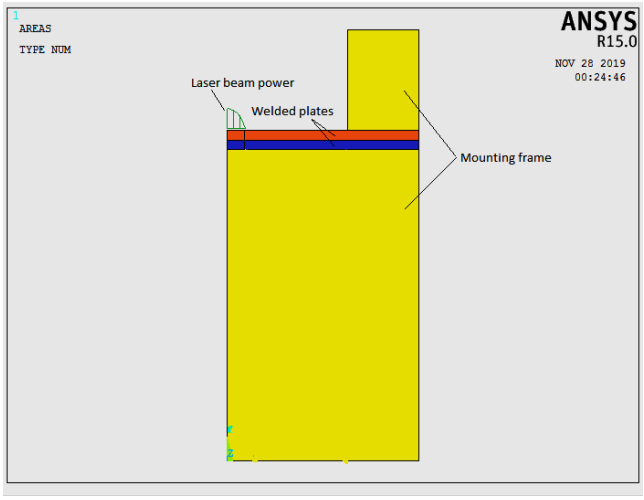

Fig. 3. Geometry of the analyzed axisymmetric section

3.3. Initial and boundary conditions

At the start of analysis (time t=0), the sheets were at room temperature. At time t>0, the following boundary conditions were applied. Gaussian heat flux q (as input power) is applied on the top surface [20].

$$q = 2q_o * \eta * e^{\left(-2*r^2/r_q^2\right)} \quad (2)$$

where q_o is heat flux at the top surface, η is material's absorptivity, r_q is the laser beam radius at the surface of the target and r is the radial distance from the laser beam center. The absorptivity of steel was set to 90% at a temperature below the boiling point [20,21]. On the other surfaces (of plates and mounting frame), that is in contact with air, heat loss boundary conditions (convection and radiation) are applied. The convection power loss on the free surfaces can be expressed as.

$$Q_c = A_s\, h(T - T_{amb}) \quad (3)$$

where Q_c convective heat flux, h convective heat transfer coefficient, T temperature of the welded sheets, T_{amb} ambient temperature. The radiation heat loss Qr is:

$$Q_r = \varepsilon\sigma\,(T^4 - T_{amb}^4) \quad (4)$$

where ε is the emissivity of the material, and σ is the Stefan-Boltzmann constant. The total heat transfer losses (convection + radiation) are determined by adding the contributions of both heat transfer mechanisms ($h_{combined} = h_{conv} + h_{rad}$) [22].

$$Q_{total} = h_{combined}\, A_s\, (T - T_{amb}) \quad (5)$$

4. Results and discussion

4.1. Weld appearance

Figure 4 illustrates the weld nugget of the samples 1 to 6, where energy is concentrated in the center of the spot. It was observed that the average diameter of the weld nugget did not exceed 1 mm for all welded samples. The symmetrical welded zone in all samples about the axis of the laser beam, proves that welding process was accomplished at best possible parameters where the heat input is uniformly distributed over the welded area.

Figure 5 illustrates the cross sections of the welded sheets: a (sample 8); b (sample 4). A big circular dip is formed for sample 8 (Fig. 5a). This attributes to excessive heat input, which led to vaporize a large amount of weld metal. Achieving a perfect joint between the overlapped welded partners requires a reasonable level of heat input and as can be seen in Figure 5b (sample 6). Welding surface cracks and porosities were not observed in any of the welds and this could be related to good crack resistance of the BM [10]. and contribution of suitable welding conditions. Figures 4 and 5 clarify a conduction laser welding mode where the weld width is higher than the weld depth [23].

4.2. Effect of laser processing parameters on joint strength

Effect of laser exposure time on joint strength

Figure 6 shows the relation between laser exposure time and tensile shear force, keeping constant power at 50 W.

Itcan be observed that the shear force value increases with gradual increasing of exposure time, which led to increasing the weld nugget diameter at sheets interface where the joint strength in lap welds is determined by the weld width at the interface [24].

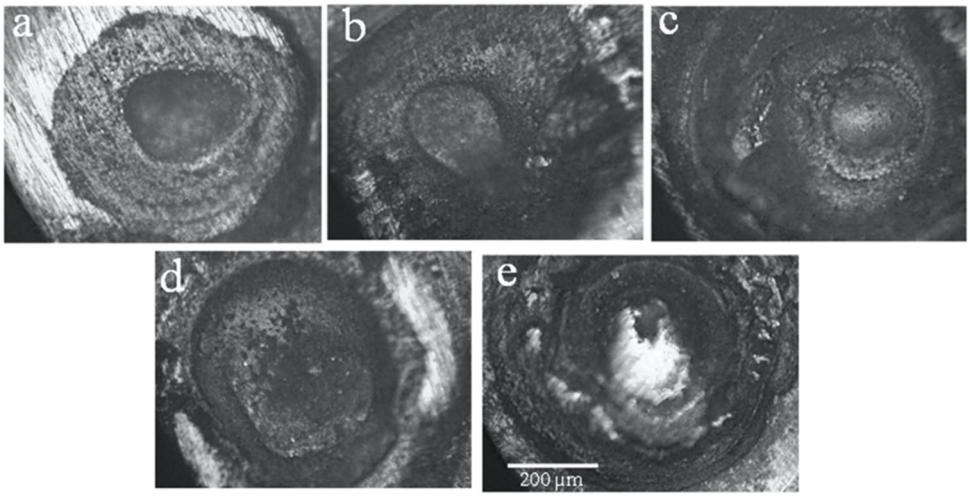

Fig. 4. Weld nugget of the overlapped samples: a (sample 2); b (sample 3); c (sample 4); d (sample 5); e (sample 6)

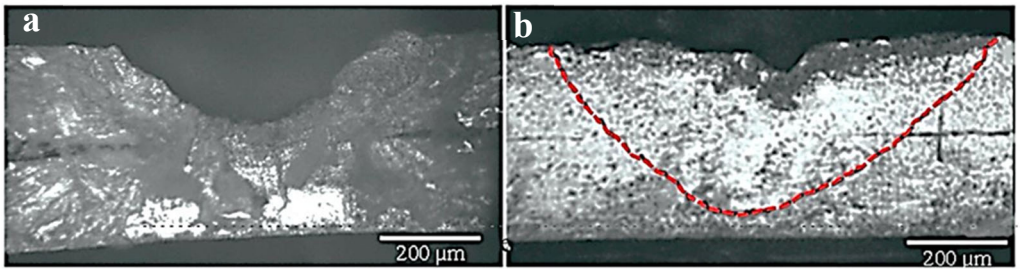

Fig. 5. Cross-sections of the weld: a (sample 8); b (sample 4)

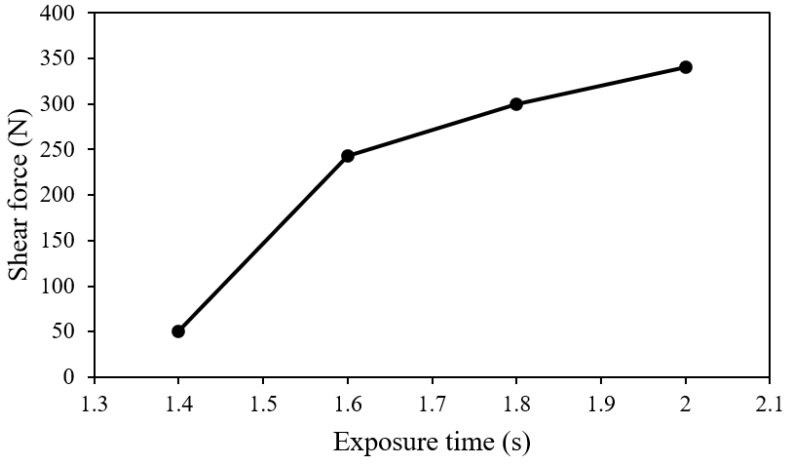

Fig. 6. Effect of laser exposure time on tensile shear force at 50 W laser power

Effect of laser power on joint strength

Figure 7 shows the relation between laser power and tensile shear force. The joint has the highest shear force at 50 (W) comparing with other laser powers. The breaking shear force of the samples starts to increase gradually till reached the maximum value (340 N) at 50 W then decreased because when power raised started to evaporate the top part of the metal surface, as shown in Figure 5a. Therefore, the strength of the joint decreased to the minimum value (80 N) at 80 W laser power.

4.3. Effect of laser processing parameters on the microhardness of the joint

Figure 8 shows the microhardness profile of sample 4 and 8. The graph shows that the weld in both samples has higher hardness values compared to the BM. The rising of hardness in the weld zone can be ascribed to the presence of carbides. In HAZ, it was found that the values of hardness were higher than the BM. This could be attributed to the high-power density welding process and thin sheet thickness that provides superior cooling rate, which eliminated the grain growth in HAZ [13,15,25]. The refined grains increase the hardness since the smaller grains provide more obstacles to dislocation motion [26,27]. It was observed that the hardness gradient across the FZ for sample 8 is higher than that of sample 4. This gave a strong prognosis that increases the laser power along 2 s period, probably encourages the carbon to diffuse and migrate from BM toward the FZ and forms more carbides.

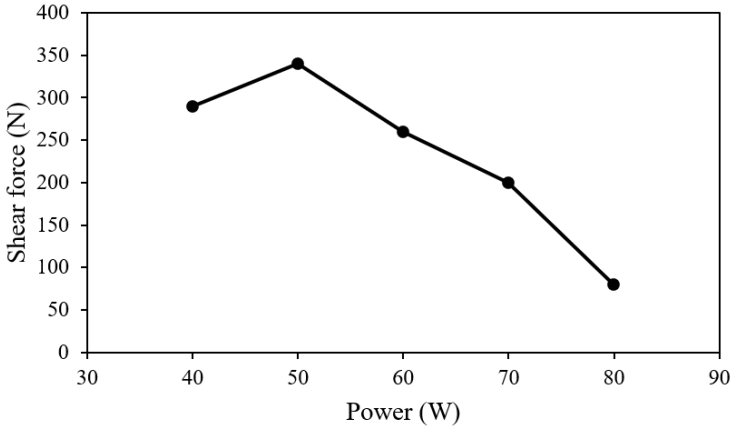

Fig. 7. Effect of laser power on tensile shear force at 2 s laser exposure time

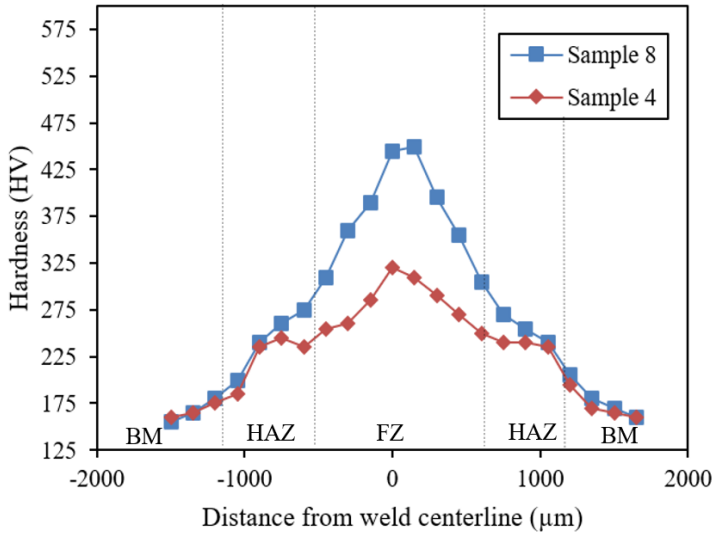

Fig. 8. Microhardness values across BM, HAZ and FZ of the joint for the samples 4 and 8

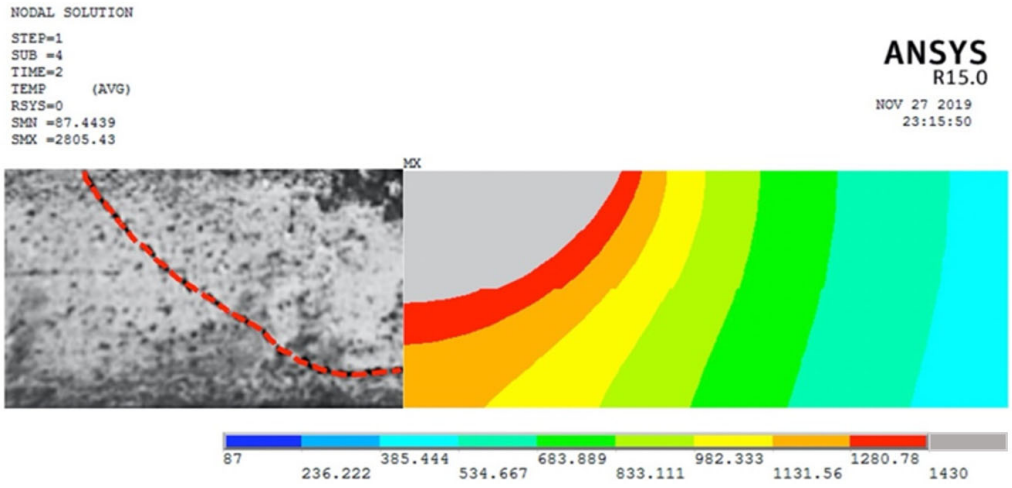

Fig. 9. Comparison between experimental (left part) and theoretical (right part) welding profiles of the welded plates at the end of laser application for the sample 4. (T_m of AISI 321 stainless steel= 1430ºC)

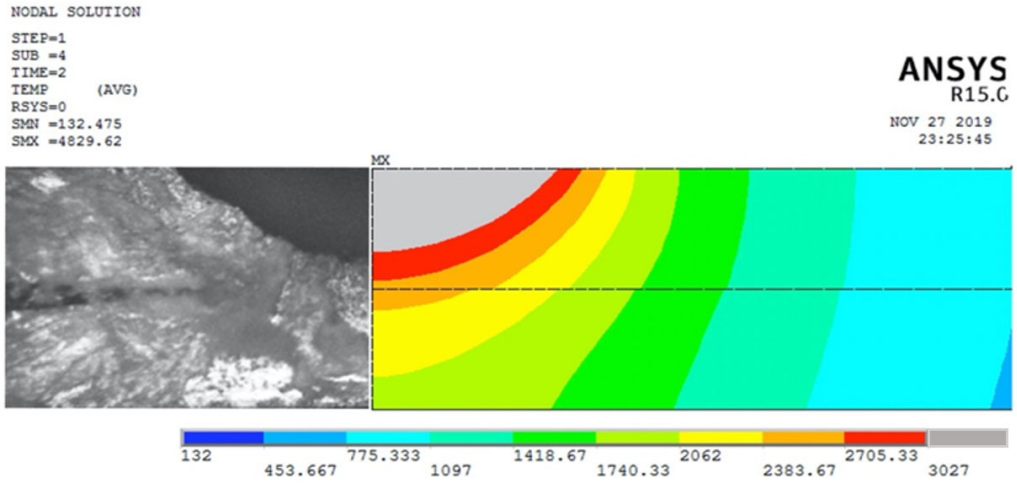

Fig. 10. Comparison between experimental (left part) and theoretical (right part) welding profiles of the welded plates at the end of laser application for the sample 8. (T_v of AISI 321 stainless steel= 3027ºC)

4.4. Finite element results

Comparison between experimental and theoretical welding profiles of the welded plates at the end of laser application is shown in Figures 9 and 10 for the samples 4 and 8 respectively. It is noticed that there is good agreement between finite element analysis with the experimental results. The accuracy of the finite element analysis depends mainly on reasonable presentation of the laser power model, and on the accurate estimation of thermal transfer resistance between contacting surface.

5. Conclusions

For the current work, the following points can be drawn:

- Thin sheets of AISI 321 of 200 μm thickness were successfully welded by LSW process.
- Welding parameters of 50W power and 2 s exposer time gave the best weld profile and highest shear breaking force.
- Highest hardness was recorded in FZ and gradually decreased towards the BM.

- The adoption of finite element analysis to the simulation of laser welding profile can provide good agreement with experimental results.

References

[1] M.V. Larin, Y.B. Pevzner, O.I. Grininand, I.T. Lasota, The use of single-mode fiber laser for welding of stainless steelthin thickness, IOP Conference Series: Journal of Physics 1109 (2018) 012036. DOI: https://doi.org/10.1088/1742-6596/1109/1/012036

[2] A. Klimpel, A. Lisiecki, T. Figiel, High power diode laser welding of austenitic steel, welding of austenitic steels, Welding International 17/3 (2003) 189-195. DOI: https://doi.org/10.1533/wint.2003.3076

[3] A. Klimpel, A. Lisiecki, M. Szczyrba, Diode Laser Welding of Duplex Steel with addition of activating flux, Welding International 17/9 (2003) 684-692. DOI: https://doi.org/10.1533/wint.2003.3196

[4] J. Adamiec, A. Grabowski, A. Lisiecki, Welding of an intermetallic Fe-Al phase-based alloy with a diode laser, Proceedings of the International Society for Optical Engineering, Laser Technology VII, Applications of Lasers 5229 (2003) 219-222. DOI: https://doi.org/10.1117/12.520720

[5] F. Bachman, Industrial applications of high power diode lasers in materials processing, Applied Surface Science 208/1 (2003) 125-136. DOI: https://doi.org/10.1016/S0169-4332(02)01349-1

[6] U. Dilthey, A. Risch, Laser welding of stainless steels and stainless low-alloy material combinations, Welding in the World 36 (1995) 135-142.

[7] Y. Tzeng, Gap-free lap welding of zinc-coated steel using pulsed CO_2 laser, International Journal of Advanced Manufacturing and Technology 29 (2006) 287-295. DOI: https://doi.org/10.1007/s00170-005-2522-3

[8] F. Curcio, G. Daurelio, F. Memola Capece Minutolo, F. Caiazzo, On the welding of different materials by diode laser, Journal of Materials Processing and Technology 175/1-3 (2006) 83-89. DOI: https://doi.org/10.1016/j.jmatprotec.2005.04.026

[9] A.A. Shehab, S.K. Sadrnezhaad, A.K. Mahmoud, M.J. Torkamany, A.H. Kokabi, M. Fakouri Hasanabadi, Pulsed Nd: YAG laser dissimilar welding of Ti/Al3105 alloys, Scientia Iranica: Transactions on Mechanical Engineering (B) 27/7 (2020) 1982-1994. DOI: https://doi.org/10.24200/SCI.2019.52217.2600

[10] ASM: Metals Handbook: Volume 1, Properties and Selection: Irons, Steels, and High-Performance Alloys, Second Edition, ASM International, USA, 1992, 150-1850.

[11] A. Klimpel, A. Lisiecki, November Laser welding of butt joints of austenitic stainless steel AISI 321 sheets 0.5 mm and 1.0 mm thick using a high power diode laser HPDL, Journal of Achievement In Materials and Manufacturing Engineering 25/1 (2007) 63-66.

[12] E.M. Stanciu, A. Pascu, M.H. Tierean, I.C. Roata, I. Voiculescu, I. Hulka, C. Croitoru, Dissimilar Laser Welding of AISI 321 and AISI 1010, Technical Gazette 25/2 (2018) 344-349. DOI: https://doi.org/10.17559/TV-20160722151049

[13] A. Hussain, A.H. Hamdani, R. Akhter, CO_2 laser welding of AISI 321stainless steel, IOP Conference Series: Materials Science and Engineering 60 (2014) 012042. DOI: https://doi.org/10.1088/1757-899X/60/1/012042

[14] W. Meng, Z. Xu, Q. Ma, X. Yin, J. Fang, Pulse fiber laser welding of AISI 321-AISI 405 stainless steel thick plates butt joints, Journal of Materials Processing Technology 271 (2019) 214-225. DOI: https://doi.org/10.1016/j.jmatprotec.2019.04.013

[15] A.A. Shehab, S.K. Sadrnezhaad, M.J. Torkamany, M. Fakouri Hasanabadi, M. Alali, A.K. Mahmoud, M.H. Abass, A.H. Kokabi, Ring-like laser spot welding of Ti grade2 to AAl3105-O using AlSiMg filler metal, Optik 206 (2020) 163630. DOI: https://doi.org/10.1016/j.ijleo.2019.163630

[16] A.K. Mahmoud, Z.A. Taha, A.A. Shehab, Temperature Distribution Simulation for Pulsed Laser Spot Welding of Dissimilar Stainless Steel AISI302 to Low Carbon Steel AISI1008, Advanced Materials Research 445 (2012) 412-417. DOI: https://doi.org/10.4028/www.scientific.net/AMR.445.412

[17] A.K. Mahmoud, Z.A. Taha, A.A. Shehab, Building a simulation model for the prediction of temperature distribution in pulsed laser spot welding of dissimilar low carbon steel 1020 to aluminum alloy 6061, American Institute of Physics Conference Proceedings 1315 (2011) 1425-1430. DOI: https://doi.org/10.1063/1.3552386

[18] J.C. Ion, Laser Processing of Engineering Materials: Principles, Procedure and Industrial Application, First Edition, 2005.

[19] W. Han, Computational and Experimental Investigations of Laser Drilling and Welding for Microelectronic Packaging, Ph.D. Thesis, Worcester Polytechnic Institute, U.S.A., 2004.

[20] A. De, S.K. Marti, C.A. Walsh, H.K.D.H. Bhadeshia, Finite Element Simulation of Laser Spot Welding,

Science and Technology of Welding and Joining 8/5 (2003) 377-384.
DOI: https://doi.org/10.1179/136217103225005570
[21] W.S. Chang, S.J. Na, A study on the prediction of the laser weld shape with varying heat source equations and the thermal distortion of a small structure in micro-joining, Journal of Material Processing Technology 120/1-3 (2002) 208-214.
DOI: https://doi.org/10.1016/S0924-0136(01)00716-6
[22] Y.A. Cengel, Heat transfer: A practical approach, McGrow Hill Inc, U.S.A. 2002.
[23] W.M. Steen, Laser Material Processing, Fourth Edition, Springer-Verlag, London, 2010.
[24] J.F. Ready, D.F. Farson, T. Feeley (eds.), LIA Handbook of Laser Materials Processing. Laser Institute of America, USA, 2001.
[25] M. Abass, M. Alali, W. Abbas, A. Shehab, Study of solidification behaviour and mechanical properties of arc stud welded AISI 316L stainless steel, Journal of Achievements in Materials and Manufacturing Engineering 97/1 (2019) 5-14.
DOI: https://doi.org/10.5604/01.3001.0013.7944
[26] H. Ming, Z. Zhang, J. Wang, E.-H. Han, W. Ke, Microstructural characterization of an SA508–309L/308L–316L domestic dissimilar metal welded safe-end joint, Materials Characterization 97 (2014) 101-115. DOI: https://doi.org/10.1016/j.matchar.2014.08.023
[27] Y. Ai, X. Shao, P. Jiang, P. Li, Y. Liu, W. Liu,Welded joints integrity analysis and optimization for fiber laser welding of dissimilar materials, Optics and Lasers in Engineering 86 (2016) 62-74. DOI: https://doi.org/10.1016/j.optlaseng.2016.05.011